PERGAMON

Acta mater. 48 (2000) 3177–3181

Acta MATERIALIA

www.elsevier.com/locate/actamat

EFFECT OF SURFACE FREE ENERGY ANISOTROPY ON DENDRITE TIP SHAPE

G. B. McFADDEN[1]†, S. R. CORIELL[1] and R. F. SEKERKA[2]

[1]National Institute of Standards and Technology, Gaithersburg, MD 20899-8910, USA and [2]Physics and Mathematics, Carnegie Mellon University, Pittsburgh, PA 15213-3890, USA

(Received 16 February 2000; accepted 14 April 2000)

Abstract—In previous work, approximate solutions were found for paraboloids having perturbations with four-fold axial symmetry in order to model dendritic growth in cubic materials. These solutions provide self-consistent corrections through second order in a shape parameter ε to the Peclet number vs supercooling relation of the Ivantsov solution. The parameter ε is proportional to the amplitude of the four-fold correction to the dendrite shape, as measured from the Ivantsov paraboloid of revolution. The equilibrium shape for anisotropic surface free energy to second order in the anisotropy is calculated. The value of ε is determined by comparing the dendrite tip shape with the portion of the equilibrium shape near the growth direction, [001], for anisotropic surface free energy of the form $\gamma = \gamma_0[1 + 4\varepsilon_4(n_1^4 + n_2^4 + n_3^4)]$, where the n_i are components of the unit normal of the crystal surface. This comparison results in $\varepsilon = -2\varepsilon_4 - 24\varepsilon_4^2 + O(\varepsilon_4^3)$, independent of the Peclet number. From the experimental value of ε_4, it is found that $\varepsilon \approx -0.012 \pm 0.004$, in good agreement with the measured value $\varepsilon \approx -0.008$ of LaCombe *et al.* (*Phys. Rev. E*, 1995, **52**, 2778) *Published by Elsevier Science Ltd on behalf of Acta Metallurgica Inc.*

Keywords: Dendritic growth; Diffusion; Phase transformations; Theory & modeling

1. INTRODUCTION

In a previous paper [1] we calculated the correction to the relationship between the Peclet number P and the dimensionless supercooling, S, for a non-axisymmetric isothermal dendrite growing from a pure supercooled melt. For four-fold axial symmetry, the dendrite shape in cylindrical coordinates (r, ϕ, z) is of the form

$$\frac{z}{\rho} = \frac{1}{2} - \frac{1}{2}\left(\frac{r}{\rho}\right)^2 - \frac{\varepsilon}{2}\cos 4\phi\left(\frac{r}{\rho}\right)^4 + \frac{\varepsilon^2}{2}\left[\alpha(P) \times \left(\frac{r}{\rho}\right)^4 + \beta(P)\left(\frac{r}{\rho}\right)^6\right] + O(\varepsilon^3) \quad (1)$$

where the shape parameter ε represents the amplitude of the four-fold perturbation to the axisymmetric paraboloid, and ρ is the radius of curvature of the dendrite tip. Specifically, $P = V\rho/2\kappa$ and $S = c_V(T_M - T_\infty)/L_V$, where V is the dendrite growth speed, κ is the thermal diffusivity of the melt, c_V is the heat capacity per unit volume, L_V is the latent heat per unit volume, T_M is the melting point, and T_∞ is the far-field temperature of the supercooled melt. The corresponding correction to the P–S relation is found to have the form

$$S = Pe^P E_1(P) + \frac{\varepsilon^2}{2}S^{(2)}(P) + O(\varepsilon^3). \quad (2)$$

The specific dependence of the coefficients α and β, and the correction $S^{(2)}$, on Peclet number are worked out in detail in Ref. [1]. Here, the function E_1 is the exponential integral [2]. For $\varepsilon = 0$ this yields the well-known result of Ivantsov [3]. Other researchers have also noted that the first-order term proportional to $r^4 \cos 4\phi$ is consistent with an isothermal solution that has been employed in microscopic solvability theory [4–7].

Based on the experimental measurements of LaCombe *et al.* [8], for succinonitrile (SCN) at $P \approx 0.004$, we estimated a value of $\varepsilon \approx -0.008$, with the convention that $\phi = 0$ corresponds to the [100] direction. The corresponding correction to S was about a 9% increase, in general agreement with the experimental results [8–11].

In this paper, we estimate the shape parameter ε theoretically on the basis of a simple idea, namely, that the shape of the isothermal but anisotropic dendrite tip is approximately the same as a portion of the equilibrium shape of an isothermal body with anisotropic surface free energy. We recognize

† To whom all correspondence should be addressed.

1359-6454/00/$20.00 Published by Elsevier Science Ltd on behalf of Acta Metallurgica Inc.
PII: S1359-6454(00)00105-1

that the equilibrium shape is a closed convex body in a strictly isothermal environment, whereas our dendrite model [1] corresponds to a semi-infinite body with an isothermal surface that is growing from a non-isothermal melt. We note, however, that an *isothermal* body, either the Ivantsov paraboloid or a perturbed paraboloid with a four-fold axial symmetry, is used to determine the underlying relationship between the Peclet number and the supercooling for all existing theoretical analyses of dendritic growth. A non-isothermal dendrite surface is only taken into account, either by invoking a marginal stability hypothesis or by conducting a microscopic solvability analysis, in order to separate the product of tip radius and growth velocity that occurs in the Peclet number. In the present analysis, we do not attempt to calculate the tip radius and growth velocity separately, but only the relationship of the shape anisotropy to the anisotropy of the surface free energy. We emphasize that a shape with variable curvature but with anisotropic surface free energy can still be isothermal, e.g. the equilibrium shape itself or, approximately, a dendrite tip. Therefore, we expect the dendrite tip *shape* to be similar to the *portion* of the equilibrium shape near the growth direction, which is [001] for SCN.

For a cubic crystal, such as SCN, we assume a surface free energy $\gamma(\hat{\mathbf{n}})$ of the form

$$\gamma = \gamma_0[1 + 4\varepsilon_4(n_1^4 + n_2^4 + n_3^4)] \tag{3}$$

where γ_0 and ε_4 are constants, and $\hat{\mathbf{n}} = (n_1, n_2, n_3)$ is the unit normal of the crystal surface. This corresponds to the leading order expansion of γ in spherical harmonics compatible with cubic symmetry; the next non-vanishing term is of sixth degree in $\hat{\mathbf{n}}$. In the subsequent analysis, we will assume that $|\varepsilon_4| \ll 1$; therefore we compute the equilibrium shape through second order in ε_4, resulting in a general formula [see equation (12)] that is of interest in a broader context.

Microscopic solvability has indicated the importance of surface free energy anisotropy in dendritic growth. However, the three-dimensional analysis of Brener and co-workers [6, 7] predicts that the shape anisotropy of the dendrite is independent of the anisotropy of surface free energy, with a value that is twice the experimental value for SCN. Thus, microscopic solvability theory predicts that the dendrite shape anisotropy ε would be the same for SCN ($\varepsilon_4 = 0.0055$ [12, 13]) and pivalic acid ($\varepsilon_4 = 0.025$ [13]) even though the latter has nearly five times larger anisotropy of surface free energy and displays dendrite morphologies that are distinctly more cruciform in shape (see, e.g. Fig. 12 of Ref. [14]).

2. ANALYSIS

2.1. Equilibrium shape

It is well known that for small anisotropy, the equilibrium shape is geometrically similar to a polar plot of the surface free energy to first order in the anisotropy [13, 15–17]. We proceed to calculate the equilibrium shape to second order in the anisotropy. A general anisotropic free energy γ can be written in the form

$$\gamma(\hat{\mathbf{n}})/\gamma_0 = 1 + 4\varepsilon_4 Q(\hat{\mathbf{n}}). \tag{4}$$

Equation (3) is a special case of equation (4) in which Q is given by

$$Q_4(\hat{\mathbf{n}}) := n_1^4 + n_2^4 + n_3^4. \tag{5}$$

We use the $\boldsymbol{\xi}$ vector formalism of Cahn and Hoffman [15] by extending the function $\gamma(\hat{\mathbf{n}})$ to a function defined in three-dimensional space by means of the prescription $\tilde{\gamma}(\mathbf{A}) := A\gamma(\mathbf{A}/A)$, where $A = |\mathbf{A}|$. Thus

$$\tilde{\gamma}(\mathbf{A})/\gamma_0 = A + 4\varepsilon_4 A\tilde{Q}(\mathbf{A}) \tag{6}$$

where $\tilde{Q}(\mathbf{A}) = Q(\mathbf{A}/A)$. Thus $\tilde{Q}(\mathbf{A})$ is a homogeneous function of degree zero in the variables A_i for $i = 1, 2, 3$, which by Euler's theorem leads to $\sum_i A_i(\partial\tilde{Q}/\partial A_i) = 0$, a relation that will be used to simplify subsequent results.

The components of the $\boldsymbol{\xi}$ vector, which are known to be proportional to the cartesian coordinates x_i of the equilibrium shape, are given by

$$\begin{aligned}\frac{x_i}{R} = \frac{\xi_i}{\gamma_0} &= \frac{\partial}{\partial A_i}\left[\frac{\tilde{\gamma}(\mathbf{A})}{\gamma_0}\right] \\ &= \frac{A_i}{A} + 4\varepsilon_4\left[\frac{A_i}{A}\tilde{Q}(\mathbf{A}) + A\frac{\partial\tilde{Q}(\mathbf{A})}{\partial A_i}\right]\end{aligned} \tag{7}$$

where R is a scale factor. The square of the spherical polar radius r_s is then given by

$$\begin{aligned}\left(\frac{r_s}{R}\right)^2 &= \frac{\sum_i x_i^2}{R^2} \\ &= 1 + 8\varepsilon_4\tilde{Q} + 16\varepsilon_4^2\left[\tilde{Q}^2 + \sum_i\left(A\frac{\partial\tilde{Q}}{\partial A_i}\right)^2\right]\end{aligned} \tag{8}$$

where the Euler theorem has been used. Expanding to second order in ε_4 gives

$$\frac{r_s}{R} = 1 + 4\varepsilon_4\tilde{Q} + 8\varepsilon_4^2\sum_i\left(A\frac{\partial\tilde{Q}}{\partial A_i}\right)^2 + O(\varepsilon_4^3). \tag{9}$$

This expression for r_s is still in terms of the coordinates of the normal vector $n_i = A_i/A$ whereas we

would like to have it in terms of the direction cosines $\alpha_i = x_i/r_s$ of the radius vector $\mathbf{r}_s$. In order to get a result for r_s that is accurate to second order in ε_4 we need to relate α_i to n_i to first order in ε_4 and then substitute into equation (9). Thus

$$\alpha_i = \frac{x_i}{r_s} = \frac{A_i}{A} + 4\varepsilon_4 A \frac{\partial \tilde{Q}}{\partial A_i} + O(\varepsilon_4^2) \tag{10}$$

and

$$\begin{aligned}\tilde{Q}(\mathbf{A}) &= \tilde{Q}(A\hat{\boldsymbol{\alpha}}) + \sum_i \frac{\partial \tilde{Q}}{\partial A_i}(A_i - A\alpha_i) + \cdots \\ &= Q(\hat{\boldsymbol{\alpha}}) - 4\varepsilon_4 \sum_i \left(A\frac{\partial \tilde{Q}}{\partial A_i}\right)^2 + O(\varepsilon_4^2).\end{aligned} \tag{11}$$

Substitution into equation (9) then gives

$$\frac{r_s}{R} = 1 + 4\varepsilon_4 Q(\hat{\boldsymbol{\alpha}}) - 8\varepsilon_4^2 \sum_i \left(A\frac{\partial \tilde{Q}}{\partial A_i}\right)^2 + O(\varepsilon_4^3) \tag{12}$$

where it is to be understood that $A_i/A = n_i$ is to be replaced by α_i in the ε_4^2 term after the differentiation is performed. Comparing equation (12) with equation (9), we note that the effect of expressing r in terms of $\hat{\boldsymbol{\alpha}}$ rather than $\hat{\mathbf{n}}$ is to change the sign of the order ε_4^2 term.

For the particular choice $Q(\hat{\mathbf{n}}) = Q_4(\hat{\mathbf{n}})$ given by equation (5), we find

$$\left[\sum_i \left(A\frac{\partial \tilde{Q}_4}{\partial A_i}\right)^2\right]_{\hat{\mathbf{n}}=\hat{\boldsymbol{\alpha}}} = 16[Q_6(\hat{\boldsymbol{\alpha}}) - Q_4^2(\hat{\boldsymbol{\alpha}})] \tag{13}$$

where

$$Q_6(\hat{\boldsymbol{\alpha}}) := \alpha_1^6 + \alpha_2^6 + \alpha_3^6. \tag{14}$$

Thus for $\gamma(\hat{\mathbf{n}})$ given by equation (4) we have

$$\begin{aligned}\frac{r_s}{R} = 1 &+ 4\varepsilon_4 Q_4(\hat{\boldsymbol{\alpha}}) - 128\varepsilon_4^2[Q_6(\hat{\boldsymbol{\alpha}}) - Q_4^2(\hat{\boldsymbol{\alpha}})] \\ &+ O(\varepsilon_4^3).\end{aligned} \tag{15}$$

In terms of the spherical polar angles Θ and Φ of the normal vector $\hat{\mathbf{n}}$, equation (3) takes the form

$$\begin{aligned}\gamma(\Theta, \Phi)/\gamma_0 = 1 &+ \varepsilon_4[4\cos^4\Theta + \sin^4\Theta(3 \\ &+ \cos 4\Phi)]\end{aligned} \tag{16}$$

and the corresponding form of equation (15) is

$$\begin{aligned}r_s/R = 1 &+ \varepsilon_4[4\cos^4\theta + (3 + \cos 4\phi)\sin^4\theta] \\ &- 8\varepsilon_4^2\{[-4\cos^3\theta\sin\theta + (3 \\ &+ \cos 4\phi)\sin^3\theta\cos\theta]^2 + \sin^2 4\phi\sin^6\theta\} \\ &+ O(\varepsilon_4^3).\end{aligned} \tag{17}$$

where θ and ϕ are the spherical polar angles of the radius vector $\mathbf{r}_s$, or of $\hat{\boldsymbol{\alpha}}$.

2.2. Dendrite tip shape

In order to compare with our dendrite shape, we must transform equation (17) to cylindrical coordinates, which we do by substituting $r_s = \sqrt{(r^2 + z^2)}$, $\cos\theta = z/\sqrt{(r^2 + z^2)}$ and $\sin\theta = r/\sqrt{(r^2 + z^2)}$ and expanding in powers of ε_4 to obtain

$$z = z_0(r) + \varepsilon_4 z_1(r, \phi) + \varepsilon_4^2 z_2(r, \phi) + O(\varepsilon_4^3) \tag{18}$$

where

$$\frac{z_0(r)}{R} = \sqrt{1 - (r/R)^2} \tag{19}$$

$$\frac{z_1(r, \phi)}{R} = \frac{4 - 8(r/R)^2 + 7(r/R)^4 + (r/R)^4\cos 4\phi}{\sqrt{1 - (r/R)^2}} \tag{20}$$

$$\begin{aligned}\frac{z_2(r, \phi)}{R} = \frac{-(r/R)^2}{2(1 - (r/R)^2)^{3/2}}\{&[144 - 864(r/R)^2 \\ &+ 1816(r/R)^4 - 1528(r/R)^6 \\ &+ 441(r/R)^8] + [-96(r/R)^2 \\ &+ 360(r/R)^4 - 384(r/R)^6 \\ &+ 126(r/R)^8]\cos 4\phi + [-8(r/R)^6 \\ &+ 9(r/R)^8]\cos^2 4\phi\}.\end{aligned} \tag{21}$$

Near the [001] direction, $|r/z| \ll 1$ so we can expand again to obtain

$$\begin{aligned}\frac{z}{R} = 1 &+ 4\varepsilon_4 - \frac{1}{2}(r/R)^2(1 + 12\varepsilon_4 + 144\varepsilon_4^2) \\ &- \frac{1}{8}(r/R)^4(1 - 36\varepsilon_4 - 2592\varepsilon_4^2) - \frac{1}{16}(r/R)^6 \\ &\times (1 - 28\varepsilon_4 + 6320\varepsilon_4^2) + (r/R)^4(\varepsilon_4 \\ &+ 48\varepsilon_4^2)\cos 4\phi + \frac{1}{2}(r/R)^6(\varepsilon_4 \\ &- 216\varepsilon_4^2)\cos 4\phi + O(|\varepsilon_4|^3, (r/R)^8).\end{aligned} \tag{22}$$

We introduce a scaling factor of the tip radius ρ

and rewrite this expression in the abbreviated form

$$\frac{z}{\rho} = -\frac{1}{2}\left(\frac{r}{\rho}\right)^2(1 + 12\varepsilon_4 + 144\varepsilon_4^2)\frac{\rho}{R} + \left(\frac{r}{\rho}\right)^4(\varepsilon_4 + 48\varepsilon_4^2)\left(\frac{\rho}{R}\right)^3\cos 4\phi + \ \ldots \tag{23}$$

where we have omitted all but the two most important terms on the right-hand side. Matching the coefficients of r^2 in equations (1) and (23) to relate the tip radius ρ to our scale factor R gives

$$\frac{\rho}{R} = \frac{1}{1 + 12\varepsilon_4 + 144\varepsilon_4^2}. \tag{24}$$

Using this expression in equating the coefficients in the terms $r^4\cos 4\phi$ in equations (1) and (23), we obtain the result

$$-\frac{\varepsilon}{2} = \varepsilon_4 + 12\varepsilon_4^2 + O(\varepsilon_4^3). \tag{25}$$

We note that there are additional terms in equation (22) that have no counterpart in equation (1). These terms arise because the equilibrium shape is a closed convex body, whereas the dendrite is a semi-infinite body. The closure of this equilibrium shape is described properly by equation (17), but is lost once one resorts to the expansion in equation (22).

2.3. *Numerical results*

We compare the approximate analytical results relating ε and ε_4 with numerical calculations for the exact equilibrium shape as described by the ξ formalism given in equation (7). For a given value of $r = r_0$, we find the relation $\Theta = \Theta(\Phi)$ such that $r(\Theta(\Phi), \Phi) = r_0$. We then obtain a parametric representation of the tip region of the form $z = z(\Phi)$ and $\phi = \phi(\Phi)$, where $\tan\phi = y(\Theta(\Phi),\Phi)/x(\Theta(\Phi),\Phi)$ defines the cylindrical angle ϕ. A periodic cubic spline is then used to obtain the relation $z = z(\phi)$ at equally spaced angles in ϕ, and the resulting function is Fourier analyzed to give

$$z = \sum_n z_n(r_0)\cos n\phi \tag{26}$$

where the Fourier coefficients z_n are functions of the prescribed value of r_0. The four-fold coefficient is expected to have leading behavior $z_4(r_0) = a_4 r_0^4 + \ \ldots$, so we define the quantity

$$\frac{-\varepsilon_c}{2} = \frac{[z_4(r_0)/\rho]}{[r_0/\rho]^4} \tag{27}$$

and compute ε_c as a function of the anisotropy coefficient ε_4 in equation (3) for various values of r_0/ρ. In Fig. 1 the solid curve shows the resulting shape parameter $-\varepsilon_c/2$ as a function of the surface tension anisotropy ε_4 for $r_0/\rho = 0.01$, which is sufficiently small that the results are independent of r_0. The dashed line is the linear approximation $-\varepsilon/2 = \varepsilon_4$, whereas the dot-dashed curve is the quadratic approximation $-\varepsilon/2 = \varepsilon_4 + 12\varepsilon_4^2$.

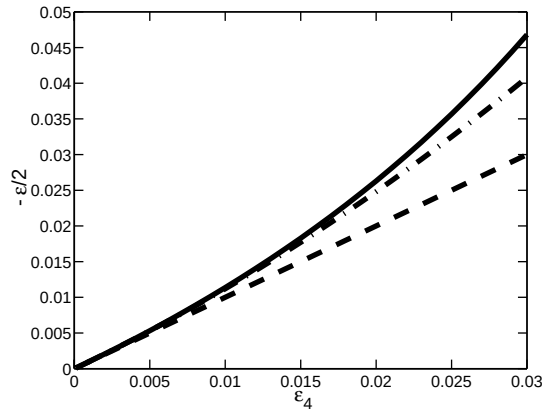

Fig. 1. The shape parameter ε as a function of the surface tension anisotropy ε_4. The dashed line is the linear approximation $-\varepsilon/2 = \varepsilon_4$, the dot-dashed curve is the quadratic approximation $-\varepsilon/2 = \varepsilon_4 + 12\varepsilon_4^2$, and the solid curve is based on a numerical calculation.

3. DISCUSSION

The anisotropy of the surface free energy for SCN has been measured by Glicksman and Singh [12] and Muschol *et al.* [13], resulting in $\varepsilon_4 = 0.0055 \pm 0.0015$, which from equation (25) yields $\varepsilon = -0.012 \pm 0.004$. This compares favorably with the direct measurements of LaCombe *et al.* [8] which result in $\varepsilon \approx -0.008$. Note, however, that the experimental determination of ε is based on measurements of the dendrite shape for distances of up to ten tip radii from the tip, whereas our comparison to the equilibrium shape is only valid within a fraction of a tip radius from the tip. Another theoretical estimate of ε has been made by Brener and co-workers [6, 7] based on microscopic solvability theory, and, in our notation, results in $|\varepsilon| = 1/48 \approx 0.02$, which is about a factor of two larger than the experimental value. Their result is independent of ε_4. By means of numerical computations based on a phase-field model, Karma and Rappel [18] calculated a shape anisotropy for $S = 0.45$ and an effective surface free energy anisotropy of 0.0066, resulting in $|\varepsilon| = 0.019$, close to the value of Brener and co-workers, and therefore still much larger than the experimental value. For a fixed supercooling of $S = 0.45$, Karma and Rappel find that $|\varepsilon|$ increases from 0.019 to 0.063 as the effective surface tension anisotropy ε_e increases from 0.0066 to 0.0470 (see Table VIII in Ref. [18]).

It therefore appears that our simple assumption that the tip anisotropy can be calculated from an

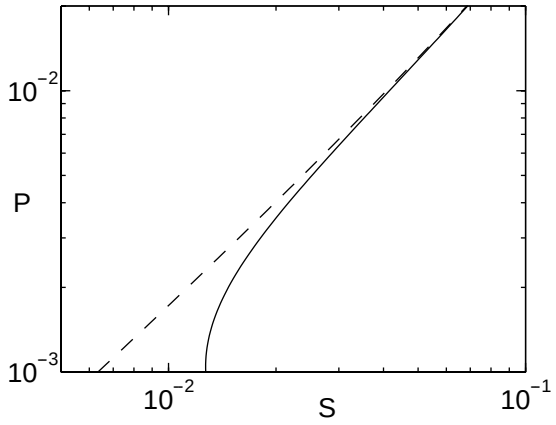

Fig. 2. The Peclet number P as a function of dimensionless supercooling S for shape parameter $\varepsilon = -0.008$ (solid curve) and $\varepsilon = 0$ (dashed curve); the dashed curve corresponds to the Ivantsov solution.

isothermal equilibrium shape is in better agreement with experiment than that calculated from solvability theory, at least for the single data point available so far for which both shape measurements and the surface energy anisotropy are available. On the other hand, the present theory does not include any assumption about the value of the actual tip temperature, so it leads only to a corrected value for the Peclet number vs supercooling. Unlike solvability theory, it makes no prediction about the separate values of tip radius and growth velocity.

A value of $\varepsilon_4 = 0.025$ has been measured for pivalic acid [13]. This anisotropy is about five times larger than that of SCN. As seen in Fig. 1, the second order expansion gives $-\varepsilon = 0.065$ for this value of ε_4, while the numerical result $-\varepsilon = 0.071$ is slightly above that value. No measurements of the actual shape anisotropy are yet available.

Note that the value of ε given by equation (25) is independent of the Peclet number P. This is supported by preliminary measurements by LaCombe [19] over a limited range of supercoolings. Accordingly, in Fig. 2 we plot the value of S from equation (2) for $\varepsilon = -0.008$. For the smaller values of P in the figure, our corrections to S are too large for our expansion in ε to be valid, resulting in a nearly vertical curve near $P = 0.001$. In the range $0.004 < P < 0.01$, our results resemble the experimental values measured by Koss *et al.*, which also lie slightly below the Ivantsov curve (see Fig. 10 of Ref. [11]). For P much below 0.004, the experimental data actually lie above the Ivantsov curve, possibly due to the effects of finite container size and/or convection [20, 21]. Thus, the effects of non-axisymmetry vs those due to finite container sizes and/or convection tend to affect S in an opposing manner.

Acknowledgements—The authors are grateful to S. A. Langer and R. J. Schaefer for helpful discussions. This work was conducted with the support of the Microgravity Research Division of NASA. R.F.S. is also grateful for support of the National Science Foundation, Grant DMR9634056.

REFERENCES

1. McFadden, G. B., Coriell, S. R. and Sekerka, R. F., *J. Cryst. Growth*, 2000, **208**, 726.
2. Abramowitz, M. and Stegun, I. A., *Handbook of Mathematical Functions*, Applied Mathematics Series 55. National Bureau of Standards, Washington, 1964.
3. Ivantsov, G. P., *Dokl. Akad. Nauk SSSR*, 1947, **58**, 567.
4. Kessler, D. A. and Levine, H., *Phys. Rev. A*, 1987, **36**, 4123.
5. Kessler, D. A. and Levine, H., *Acta metall.*, 1988, **36**, 2693.
6. Ben Amar, M. and Brener, E., *Phys. Rev. Lett.*, 1993, **71**, 589.
7. Brener, E. and Mel'nikov, V. I., *JETP*, 1995, **80**, 341.
8. LaCombe, J. C., Koss, M. B., Fradkov, V. E. and Glicksman, M. E., *Phys. Rev. E*, 1995, **52**, 2778.
9. Glicksman, M. E., Koss, M. B., Bushnell, L. T., LaCombe, J. C. and Winsa, E. A., *ISIJ Int.*, 1995, **35**, 604.
10. Koss, M. B., Bushnell, L. T., LaCombe, J. C. and Glicksman, M. E., *Chem. Engng Commun.*, 1996, **152–153**, 351.
11. Koss, M. B., LaCombe, J. C., Tennenhouse, L. A., Glicksman, M. E. and Winsa, E. A., *Metals Mater. Trans.*, 1999, **30A**, 3177.
12. Glicksman, M. E. and Singh, N. B., in *Rapidly Solidified Powder Aluminum Alloys*, ed. M. E. Fine and E. A. Starke Jr. ASTM, Philadelphia, 1986, p. 44.
13. Muschol, M., Liu, D. and Cummins, H. Z., *Phys. Rev. A*, 1992, **46**, 1038.
14. Glicksman, M. E. and Marsh, S. P., in *Handbook of Crystal Growth*, Vol. 1B, ed. D. T. J. Hurle. North-Holland, Amsterdam, 1993, p. 1104.
15. Cahn, J. W. and Hoffman, D. W., *Acta metall.*, 1974, **22**, 1205.
16. Voorhees, P. W., Coriell, S. R., McFadden, G. B. and Sekerka, R. F., *J. Cryst. Growth*, 1984, **67**, 425.
17. Coriell, S. R. and McFadden, G. B., in *Handbook of Crystal Growth*, Vol. 1B, ed. D. T. J. Hurle. Elsevier, Amsterdam, 1993, pp. 785–857.
18. Karma, A. and Rappel, W.-J., *Phys. Rev. E*, 1998, **57**, 4342.
19. LaCombe, J. C., Ph.D. thesis, Department of Materials Science and Engineering, Rensselaer Polytechnic Institute, Troy, NY, December 1998.
20. Pines, V., Chait, A. and Zlatkowski, M., *J. Cryst. Growth*, 1996, **167**, 383.
21. Sekerka, R. F., Coriell, S. R. and McFadden, G. B., *J. Cryst. Growth*, 1997, **171**, 303.